http://dx.doi.org/10.14500/aro.10843

Preparation and Characterization of Green Fe_3O_4 Nanoparticle Using the Aqueous Plant Extract of *Gundelia tournefortii* L.

Aveen F. Jalal, Nabil A. Fakhre

Department of Chemistry, College of Education, Salahaddin University-Erbil,
Erbil, Kurdistan Region - F.R. Iraq

***Abstract*—In this work, the magnetite nanoparticles (Fe_3O_4-NPs) synthesized using a simple, fast, and environmentally acceptable green approach. *Gundelia tournefortii* L. extract, an aqueous plant extract, was used for the 1st time in green synthesis to prepare nanoparticles as reducing, capping, and stabilizing agents. Such biomolecules as flavonoids, alkaloids, and antioxidants are found in the aqueous leaf extract, and their presence has been determined to have an important role in the synthesis of Fe_3O_4-NPs. The techniques used in this analysis include Fourier Transform Infrared, Scanning Electron Microscopy, Energy-Dispersive X-ray spectroscopy, X-ray Diffraction, Transmission Electron Microscopy, and Vibrating Sample Magnetometer. The Vibrating Sample Magnetometer demonstrated that the samples were superparamagnetic, with a magnetization value of 48.6 emu/g. The prepared nanoparticle was applied to remove chrystal violet, malachite green, and safranin dyes from prepared aqueous solutions with the adsorption capacity of 13.9, 15.6, and 14.4 mg/g, respectively.**

***Index Terms*—Green synthesis; *Gundelia tournefortii* L. leaf extract; Fe_3O_4 nanocomposite; Characterization.**

I. Introduction

Iron nanoparticles have generated a lot of interest in ecological research due to their great surface sensitivity and huge surface area; moreover, pathogenic microorganisms, organic pollutants, and inorganic toxins are all eliminated in ecological studies. There are plethoras of physical, chemical, biological, and hybrid techniques available for synthesizing various kinds of nanoparticles, and the nanoparticles generated by each process have certain characteristics. However, there is currently the development of metal nanoparticles production by plants. Green nanotechnology has been drawn by a broad variety of procedures to decrease or remove toxic substances for environmental restoration. A modern approach for their production is to synthesize metal nanoparticles by utilizing inactivated tissues, plant extracts, exudates, and other components (Kanagasubbulakshmi and Kadirvelu, 2017). To avoid the toxic and flammable sodium borohydride, which is used as a reducing agent, scientists are working at green preparations of iron nanoparticles. Furthermore, because no harmful chemicals are employed during the preparation of plant extracts as a reducing agent, they are suitable for biomedical and pharmaceutical applications. Recently, a significant amount of research on iron nanoparticles have been published that use plant extracts for producing green iron nanoparticles (Da'na, Taha and Afkar, 2018). *Gundelia tournefortii* L. (GT), an edible spiky, thistle-like plant native to Iran, Iraq, Turkey, Azerbaijan, Egypt, Cyprus, Jordan, and other parts of Western Asia, is locally known as "Kangar" in Iran and the Kurdistan region of Iraq. Galgal, Tumbleweed, Tumble Thistle, Akkub, and Akoub are among the most common names for GT For a long time, the plant's stem has been used as a hepatoprotective purifier and as a possible cure for diabetes, chest discomfort, and heart attacks in traditional medicine in the Middle East (Hajizadeh-Sharafabad, et al., 2016). Phytochemical analysis of GT leaves revealed the presence of phenolic compounds, particularly flavonoids, including caffeoylquinic acid derivatives, quercetin, gallic acid, and other phytoconstituents, namely, total alkaloids, ascorbic acid, reducing power, total antioxidant activity, and metal chelating activity (Ibrahim, Jalal and Ibrahim, 2013). An aqueous extract of white tea (*Camellia sinensis*) was used as a reducing and capping agent to prepare iron oxide magnetic nanoparticles (Shojaee and Shahri, 2016). For the first time, the influence of *Glycosmis mauritiana* leaf extract on the synthesis of iron oxide nanoparticles (Fe_2O_3 NPs) was investigated, as well as the efficacy of *G. mauritiana* leaves as a biomaterial as a reducing agent (Amutha and Sridhar, 2018). Iron Fe_2O_3 NPs were synthesized in a green way by extracting pomegranate (*Punica granatum*) seeds (Bibi, et al., 2019). Mango peel extracts were used to effectively manufacture GMP-nZVI (Desalegn, et al., 2019). The treatment of ferrous and ferric salt aqueous solutions in an alkaline medium with *Myrtus communis* L. leaf extract resulted in the rapid production of Fe_3O_4-NPs (Saleh, 2020). As far as we know, this is the first study used in the biosynthesis of Fe_3O_4-NPs of inexpensive GT raw extract for probable hyperthermia. X-ray powder diffraction

ARO-The Scientific Journal of Koya University
Vol. IX, No.2 (2021), Article ID: ARO.10843, 6 pages
DOI: 10.14500/aro.10843
Received: 26 July 2021; Accepted: 13 November 2021
Regular research paper: Published: 01 December 2021
Corresponding author's e-mail: aveen.jalal@su.edu.krd

(XRD), transmission electron microscopy (TEM), scanning electron microscope (SEM), energy-dispersive X-ray spectroscopy, vibrating sample magnetometer (VSM), and Fourier-transform infrared (IR) spectroscopy are used in the analysis of the present research. The prepared nanoparticle was applied to remove chrystal violet (CV), malachite green (MG), and Safranin (S) dyes from prepared aqueous solutions.

II. Material and Methods

A. Reagents

All chemicals used in the present work are in reagent grade, namely, Iron(III) Chloride Hexahydrate ($FeCl_3.6H_2O$) (Sigma-Aldrich), Iron(II) Sulfate-heptahydrate ($FeSO_4 \cdot 7H_2O$) (Sigma-Aldrich), Sodium hydroxide (NaOH) (Scharlau), and Ethanol (Sigma-Aldrich). Deionized distilled water and distilled water were obtained from our analytical laboratory.

B. Preparation of Plant Extract

Fig. 1 shows a photo of GT (Family name, Asteraceae and Local name, Kangir) from the mountains of Kurdistan region, Iraq. After collecting, the specimens were thoroughly cleaned to remove particles of dust so that any remaining moisture could be removed. The plant was left to dry in a shady, well-ventilated area; it was sliced into small parts and then transferred into a thin powder, depending on how the plant is harvested with some modifications (Ramesh, et al., 2018, Sravanthi, Ayodhya and Swamy, 2019). To prepare the solution, 5 g of the powdered plant was put into a conical flask containing 100 ml of deionized H_2O. After 15 min of heating at 60°C, the extract was filtered on Whatman's No.1 filter paper. The pale brown filtrate was kept at a 4°C temperature.

C. Synthesis of Fe_3O_4 NPs

Iron Fe_2O_3 NPs were prepared, firstly, 20 ml of 2.0 M of $FeCl_3.6H_2O$ solution and 20 ml of 1.0 M of $FeSO_4.7H_2O$ solution (2:1 molar ratios), then it was added into a 100 ml of plant extract solution. The solution was then added dropwise to 1.0 M NaOH while stirring continuously. The solution's pH was adjusted to 11. It was agitated for 1.0 h to ensure homogeneity and to complete the reaction. The Fe_3O_4-NPs were separated using magnet, as shown in Fig. 2. Fe_3O_4-NPs were cleaned several times by ethanol, and deionized distilled water. The nanoparticles were dried for 24 h at a 70°C temperature.

Fig. 1. Image of *Gundelia tournefortii* L.

D. Characterization of Fe_3O_4 NPs

PANalytical X'Pert X-ray diffractometer was utilized to examine the crystal structure and purity of the produced adsorbents. To prepare the sample for testing, it was scanned using Cu Kα radiation (λ = 1.54 Å) at 2θ angle configuration scanning from 20° to 80°, with an applied current of 40 mA and a voltage of 45 kV. Fourier transform IR (FT-IR) spectroscopy was recorded on SHIMADZU IR AFFINITY-I FTIR spectrophotometer to study the presence of the biomolecules, which are responsible for the synthesis of Fe_3ONPs. Dried samples were grinded with potassium bromide to produce a pellet, which was examined in a wavelength range of 400–4000 cm^{-1}. Surface shape, morphology, and elemental composition of materials were obtained using SEM (SEM Compact 6073) and energy dispersive X-ray analysis (EDX) (Merlin Compact 6073) (Carl Zeiss, Germany). The size and morphology of the synthesized Fe_3O_4 NPs were observed using the FEI TECNAI G2 F20 TEM. Measurement of the magnetic properties of the nanoparticles was done in a VSM produced by Daghigh Kavir Corporation at room temperature.

III. Results and Discussion

A. FTIR

FT-IR spectra of synthesized magnetic nanoparticles were carried out to identify the possible biomolecules responsible for the capping and stabilization of nanoparticles. As shown in Fig. 3, the stretching vibrations are at 3409 cm^{-1}, 1587 cm^{-1}, 1097 cm^{-1} and 615 cm^{-1} within the region of 400–4000 cm^{-1}. These peaks represent the following bonding in the sample that confirms the reducing agent role in the formation of Fe_3O_4 -NPs. The peak at 3409 cm^{-1} corresponds to the O-H stretching vibration in OH-groups,

Fig. 2. Magnetite nanoparticles separated by using an external magnetic field.

http://dx.doi.org/10.14500/aro.10843

which indicates the aqueous phase as well as the reduction of the Iron salts. The peaks at 1587 cm^{-1} and 1097 cm^{-1} attributed to the asymmetric and symmetric stretching vibration to the C=O, and C-O bond stretching denotes the existing phytochemicals in the plant extract which stabilize as well as act as capping agents (Awwad and Salem, 2012). Fe-O stretching vibration is attributed to the band below 700 cm^{-1}. The Fe-O stretching band of Fe_3O_4 nanoparticles can be detected at 615 cm^{-1} (Sobh, Nasr and Mohamed, 2020, Sari and Yulizar, 2017, Kanagasubbulakshmi and Kadirvelu, 2017).

B. SEM

Visual inspection of the surface using SEM analysis was carried out to discern morphological features, shape, and distribution of the nanoparticles' size, as illustrated in Fig. 4. As shown, GT extraction reveals the spherical with some hexagonal-shaped crystalline structure of Fe_3O_4 in the SEM micrograph of magnetic iron Fe_2O_3 NPs; it can be found that, given of high surface energy and adherence, most particles are approximately spherical with some hexagonal-shaped (Ardelean, et al., 2017) (Alzaidi, Alzahrani and El-Mouhty, 2016).

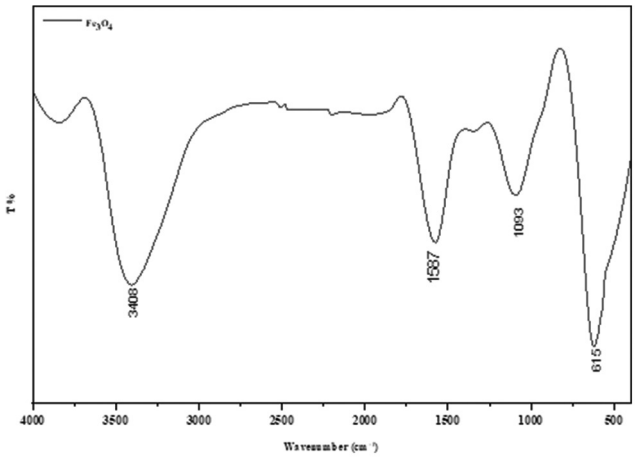

Fig. 3. Fourier transform infrared spectra Fe_3O_4 nanoparticles.

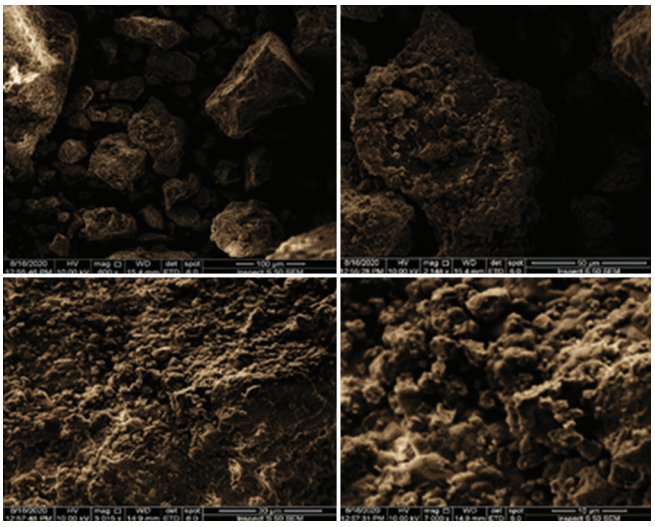

Fig. 4. Scanning electron microscope images of the biosynthesized iron oxide nanoparticles.

C. EDX

EDX analysis was used to perform qualitative analysis of prepared nanoparticles (Fig. 5), which indicates the presence oxygen and Iron elements in the composition of magnetite nanoparticles (Fe3O4-NPs) prepared from an aqueous plant extract of GT The iron and oxygen atoms in Fe3O4-NPs are stoichiometric to each other, the theoretical and experimental values are in agreement. The presence of a significant amount of iron ions inside these nanoparticles highlights the effective production of Fe3O4-NPs using the plant (Saleh, 2017) (Ahmadi, et al., 2020).

D. TEM

The size and morphology of the synthesized Fe_3O_4 nanoparticles were measured using TEM imaging. The Fe_3O_4 nanoparticles are nanocrystalline, as seen in Fig. 6, though their shape is mostly spherical with some hexagonal-shaped nanoparticles (Nejati-Koshki, et al., 2014, Yew, et al., 2016). The average particle size of the spherical nanoparticles is 29.9 nm. Moreover, Fe_3O_4 nanoparticles are agglomerations in some areas. The presence of agglomeration might be due to van der Waals forces that bind particles together, as well as nanoscale shear forces. Furthermore, the presence of

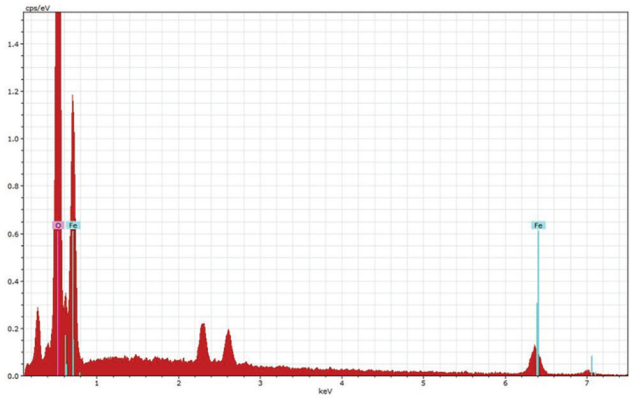

Fig. 5. Energy dispersive X-ray analysis spectrum of iron oxide nanoparticles.

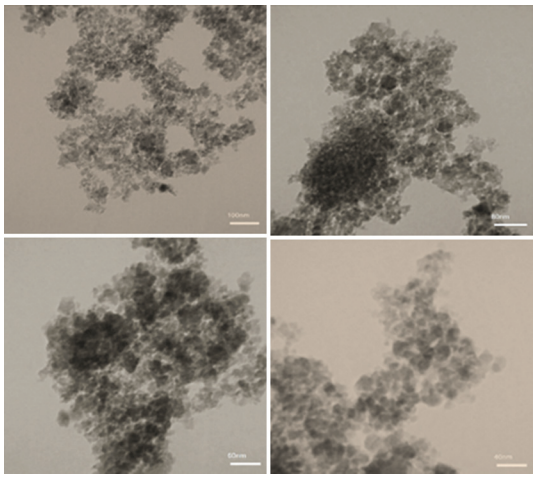

Fig. 6. Transmission electron microscopy images of the synthesized magnetite nanoparticles by *Gundelia tournefortii* L extraction.

hydroxyl groups in plant extracts may cause agglomeration (Yusefi, et al., 2021).

TABLE I
REMOVAL PERCENT OF DYES

Fe_3O_4-NPs	
Dyes	Removal %
MG	78
CV	69.5
S	72

CV: Chrystal violet, MG: Malachite green, S: Safranin

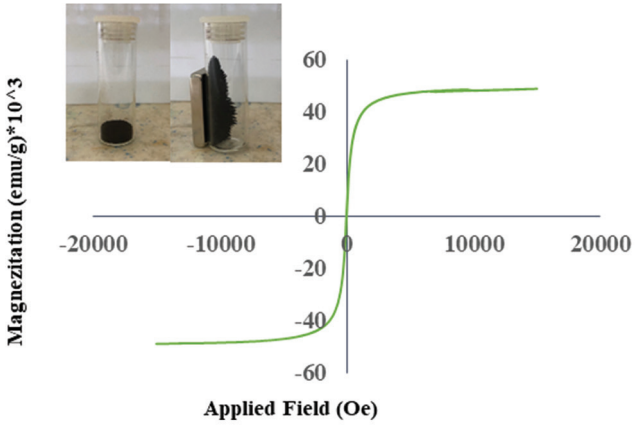

Fig. 7. Vibrating-sample magnetometry diagrams for magnetite nanoparticles.

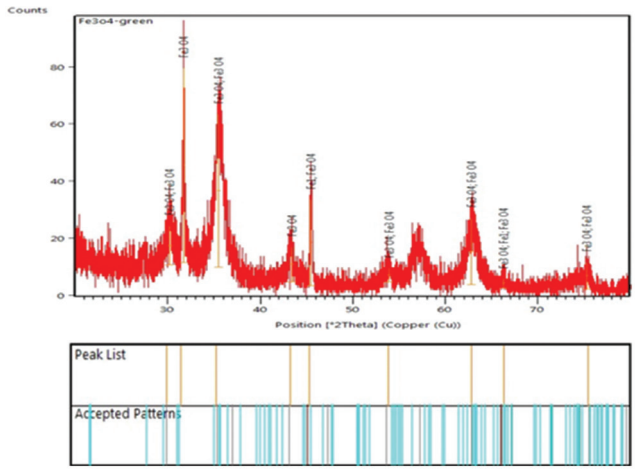

Fig. 8. X-ray powder diffraction patterns of iron oxide nanoparticles.

E. VSM

One of the expected features of the synthesized nanoparticles in this study is magnetic properties. Magnetometry technique was used to measure the magneto-resistance impact of nanoparticle-generated magnetic characteristics in the field of 20,000–20,000 at room temperature. Fig. 7 shows that the iron Fe_2O_3 NPs prepared using GT extraction are superparamagnetic, with saturation magnetization value of 48.6 emu/g being established by measuring magnetic hysteresis curves. Saturation magnetization values for Fe_3O_4 nanoparticles prepared by this plant were higher than those Fe_3O_4 nanoparticles prepared by other researches in literature (Zhen, et al., 2011, Deshmukh, Gupta and Kim, 2019).

F. XRD

Fig. 8 shows the XRD pattern of Fe_3O_4-NPs prepared using extraction of GT These peaks reflect the amorphous structure (220), (311), (400), (442), (511), (440) of iron oxide. Moreover, the rhombohedral structure of iron oxide may be indexed to all of the reflection peaks (JCPDS NO. 89-8104). Similar to iron Fe_2O_3 NPs, these studies describe a crystalline form (Amutha and Sridhar, 2018; Ahmadi, et al., 2021). The typical crystalline size of Fe_3O_4 nanoparticles, according to the dominant peak (311) diffraction peak, is 15.17 nm as expected by Scherrer's equation: $D311 = \frac{0.94\lambda}{\beta Cos\theta(311)}$, where D311 is the usual crystallographic dimension normal to the (311) crystal plane, λ is the X-ray wavelength (1.5406 Å), and β is the full width at half maximum of the (311) plane (Barzinjy, et al., 2020). The crystalline size was 29.6 nm, according to the results. The crystallite size of the Fe3O4-NPs formed varied between 11.7 mn and 69.3 nm, according to the XRD study (Yew, et al., 2016).

IV. APPLICATIONS

Fe_3O_4 nanoparticles have been applied to remove CV, MG, and S dyes from syntheses solution, as can be seen in Fig. 9. The optimum conditions for removal of 10 µg/mL dyes were 50 mg of nanoparticles with natural pH 5.5 at room temperature, and one hour shaking in thermostat shaker water bath after separating adsorbent to adsorbate using an external magnet and the residue measured with a ultraviolet-visible spectrophotometer. Results had been illustrated in Table 1 and Fig. 10. Table 2 shows that the adsorption capacity of MG, S, and CV is comparable to various adsorbents reported in the literature.

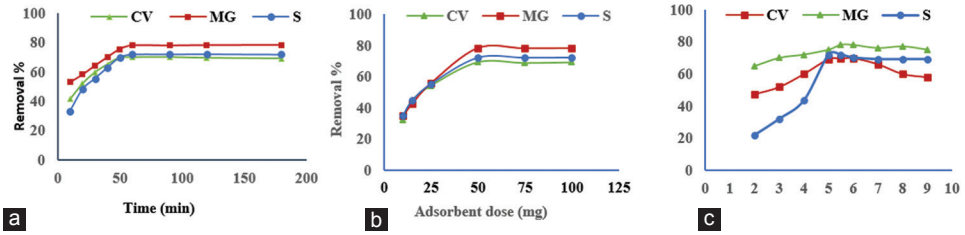

Fig. 9. (a) Adsorption time impact of chrystal violet, malachite green, and safranin removal, (b) Adsorbent dose effect on percent removal of chrystal violet, malachite green, and safranin, and (c) pH Effect on removal percentage.

http://dx.doi.org/10.14500/aro.10843

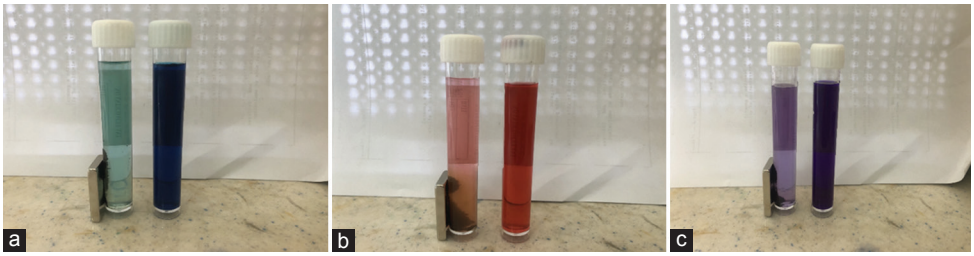

Fig. 10. Magnetite nanoparticles applied of Dyes (a) malachite green, (b) safranin and (c) chrystal violet.

Table II
Comparison of CV, MG and S Adsorbent in Different Adsorbent Materials

Adsorbents	Dyes	Adsorption capacity (mg/g)	References
Sagaun sawdust		3.5	(Khattri and Singh, 2012)
(PNIPAm) nanocomposite (CPN) hydrogels		1.2	(Zhang, et al., 2014)
$CaFe_2O_4$ magnetic nanoparticles (MNPs)		10.68	(An, et al., 2015)
Clay/poly (N-isopropyl acrylamide)			
Magnetite Alginate		37.5	(Elwakeel, et al., 2017)
BC-PKS		24.45	(Kyi, et al., 2020)
Fe_3O_4-NPs		13.9	This study
Fly ash		0.219-0.644	(Khan, et al., 2009)
Neem sawdust (Azadirachta indica)		4.354	(Khattri and Singh, 2009)
Orange peel		1.744	(Abdurrahman, et al., 2013)
Activated Carbon (AC)		28.8	(Lam, et al., 2017)
Fe_3O_4-NPs		15.6	This study
Natural Raw Kaolinite (NRK) clay		15.6	(Adebowale, et al., 2014)
Pineapple peels		21.7	(Mohammed, et al., 2014)
Iron oxide/sepiolite magnetite composite		18.48	(Fayazi, et al., 2015)
Tea waste powder		14.814	(Nehaba, et al., 2019)
Activated Carbon		20.04	(Nehaba, et al., 2019)
Fe_3O_4-NPs		14.4	This study

CV: Chrystal violet, MG: Malachite green, S: Safranin, Fe_3O_4-NPs: Magnetite nanoparticles

V. Conclusion

Fe_3O_4 nanoparticles were successfully synthesized through the green method of utilizing aqueous plant extracts of GT, as characterized by FT-IR, XRD, EDX, SEM, TEM, and VSM techniques. The photochemical present in aqueous leaf extract of GT can act as a reducing, stabilizing, and capping agent for the preparation of megnatied Fe_3O_4-NPs. The average particle size of the particles was measured at 29.9 nm. The magnetic Fe_3O_4 nanoparticles in magnetization curve illustrates their superparamagnetic characteristics at room temperature, with a magnetization value of 48.6 emu/g. The prepared nanoparticle was successfully applied to remove CV, MG, and S dyes from prepared aqueous solutions with the adsorption capacity of 13.9, 15.6, and 14.4 mg/g, respectively.

References

Abdurrahman, F.B., Akter, M. and Abedin, M.Z., 2013. Dyes removal from textile wastewater using orange peels. *International Journal of Scientific and Technology Research*, 2, pp.47-50.

Adebowale, K.O., Olu-Owolabi, B.I. and Chigbundu, E.C., 2014. Removal of safranin-O from aqueous solution by adsorption onto kaolinite clay. *Journal of Encapsulation and Adsorption Sciences*, 4, p.89.

Ahmadi, S., Fazilati, M., Mousavi, S.M. and Nazem, H., 2020. Anti-bacterial/fungal and anti-cancer performance of green synthesized Ag nanoparticles using summer savory extract. *Journal of Experimental Nanoscience*, 15, pp.363-380.

Ahmadi, S., Fazilati, M., Nazem, H. and Mousavi, S.M., 2021. Green synthesis of magnetic nanoparticles using Satureja hortensis essential oil toward superior antibacterial/fungal and anticancer performance. *BioMed Research International,* 2021, p.8822645.

Alzaidi, J., Alzahrani, E. and El-Mouhty, N., 2016. Chemical studies on the preparation of magnetic nanoparticles coated with glycine and its application for removal of heavy metals. *Oriental Journal of Chemistry*, 32, pp.1503-1513.

Amutha, S. and Sridhar, S., 2018. Green synthesis of magnetic iron oxide nanoparticle using leaves of *Glycosmis mauritiana* and their antibacterial activity against human pathogens. *Journal of Innovations in Pharmaceutical and Biological Sciences*, 5, pp.22-26.

An, S., Liu, X., Yang, L. and Zhang, L., 2015. Enhancement removal of crystal violet dye using magnetic calcium ferrite nanoparticle: Study in single-and binary-solute systems. *Chemical Engineering Research and Design*, 94, pp.726-735.

Ardelean, I.L., Stoencea, L.B.N., Ficai, D., Ficai, A., Trusca, R., Vasile, B.S., Nechifor, G. and Andronescu, E., 2017. Development of stabilized magnetite nanoparticles for medical applications. *Journal of Nanomaterials*, 2017, p.6514659.

Awwad, A.M. and Salem, N.M., 2012. A green and facile approach for synthesis of magnetite nanoparticles. *Nanoscience and Nanotechnology*, 2, pp.208-213.

Barzinjy, A.A., Abdul, D.A., Hussain, F.H. and Hamad, S.M., 2020. Green synthesis of the magnetite (Fe3O4) nanoparticle using Rhus coriaria extract: A reusable catalyst for efficient synthesis of some new 2-naphthol bis-Betti bases. *Inorganic and Nanometal Chemistry*, 50, pp.620-629.

Bibi, I., Nazar, N., Ata, S., Sultan, M., Ali, A., Abbas, A., Jilani, K., Kamal, S., Sarim, F.M. and Khan, M.I., 2019. Green synthesis of iron oxide nanoparticles

using pomegranate seeds extract and photocatalytic activity evaluation for the degradation of textile dye. *Journal of Materials Research and Technology*, 8, pp.6115-6124.

Da'na, E., Taha, A. and Afkar, E., 2018. Green synthesis of iron nanoparticles by *Acacia nilotica* pods extract and its catalytic, adsorption, and antibacterial activities. *Applied Sciences*, 8, p.1922.

Desalegn, B., Megharaj, M., Chen, Z. and Naidu, R., 2019. Green synthesis of zero valent iron nanoparticle using mango peel extract and surface characterization using XPS and GC-MS. *Heliyon*, 5, p.e01750.

Deshmukh, A.R., Gupta, A. and Kim, B.S., 2019. Ultrasound assisted green synthesis of silver and iron oxide nanoparticles using fenugreek seed extract and their enhanced antibacterial and antioxidant activities. *BioMed Research International*, 2019, p.1714358.

Elwakeel, K.Z., El-Bindary, A., El-Sonbati, A. and Hawas, A.R., 2017. Magnetic alginate beads with high basic dye removal potential and excellent regeneration ability. *Canadian Journal of Chemistry*, 95, p.807-815.

Fayazi, M., Afzali, D., Taher, M., Mostafavi, A. and Gupta, V., 2015. Removal of Safranin dye from aqueous solution using magnetic mesoporous clay: Optimization study. *Journal of Molecular Liquids*, 212, pp.675-685.

Hajizadeh-Sharafabad, F., Alizadeh, M., Mohammadzadeh, M.H.S., Alizadeh-Salteh, S. and Kheirouri, S., 2016. Effect of *Gundelia tournefortii* L. extract on lipid profile and TAC in patients with coronary artery disease: A double-blind randomized placebo controlled clinical trial. Journal of Herbal Medicine, 6, pp.59-66.

Ibrahim, G.I., Jalal, A.F. and Ibrahim, B.M., 2013. Evaluation of antioxidant activity, phenolic, flavonoid and ascorbic acid. *Tikrit Journal of Pure Science*, 18, p.3.

Kanagasubbulakshmi, S. and Kadirvelu, K., 2017. Green synthesis of iron oxide nanoparticles using Lagenaria siceraria and evaluation of its antimicrobial activity. *Defence Life Science Journal*, 2, pp.422-427.

Khan, T.A., Ali, I., Singh, V.V. and Sharma, S., 2009. Utilization of fly ash as low-cost adsorbent for the removal of methylene blue, malachite green and rhodamine B dyes from textile wastewater. *Journal of Environmental Protection Science*, 3, p.11-22.

Khattri, S. and Singh, M., 2009. Removal of malachite green from dye wastewater using neem sawdust by adsorption. *Journal of Hazardous Materials*, 167, p.1089-1094.

Khattri, S. and Singh, M., 2012. Use of Sagaun sawdust as an adsorbent for the removal of crystal violet dye from simulated wastewater. *Environmental Progress and Sustainable Energy,* 31, pp.435-442.

Kyi, P.P., Quansah, J.O., Lee, C.G., Moon, J.K. and Park, S.J., 2020. The removal of crystal violet from textile wastewater using palm kernel shell-derived biochar. *Applied Sciences*, 10, p.2251.

Lam, S.S., Liew, R.K., Wong, Y.M., Yek, P.N.Y., Ma, N.L., Lee, C.L. and Chase, H.A., 2017. Microwave-assisted pyrolysis with chemical activation, an innovative method to convert orange peel into activated carbon with improved properties as dye adsorbent. *Journal of Cleaner Production*, 162, pp.1376-1387.

Mohammed, M., Ibrahim, A. and Shitu, A., 2014. Batch removal of hazardous safranin-O in wastewater using pineapple peels as an agricultural waste based adsorbent. *International Journal of Environmental Monitoring and Analysis,* 2, pp.128-133.

Nehaba, S.S., Abdullah, R.H., Oda, A.M., Omran, A.R. Mottaleb, A.S., 2019. Evaluation of the efficiency of tea waste powder to remove the Safranin O dye compared to the activated carbon as adsorbent. *Oriental Journal of Chemistry*, 35, p.1201.

Nejati-Koshki, K., Mesgari, M., Ebrahimi, E., Abbasalizadeh, F., Fekri Aval, S., Khandaghi, A.A., Abasi, M. and Akbarzadeh, A., 2014. Synthesis and *in vitro* study of cisplatin-loaded Fe3O4 nanoparticles modified with PLGA-PEG6000 copolymers in treatment of lung cancer. *Journal of Microencapsulation*, 31, pp.815-823.

Ramesh, A., Rama Devi, D., Mohan Botsa, S. and Basavaiah, K., 2018. Facile green synthesis of Fe3O4 nanoparticles using aqueous leaf extract of *Zanthoxylum armatum* DC. for efficient adsorption of methylene blue. Journal of Asian Ceramic Societies, 6, pp.145-155.

Saleh, H.I., 2017. *Green Synthesis of Magnetite Nanoparticles using Myrtus communis* L. Grown in Egypt, Egypt.

Saleh, H.I., 2020. Green Synthesis of Magnetite Nanoparticles using *Myrtus communis* L. Grown in Egypt, Egypt.

Sari, I. and Yulizar, Y., 2017. *Green Synthesis of Magnetite (Fe3O4) Nanoparticles using Graptophyllum pictum Leaf Aqueous Extract*. IOP Conference Series: Materials Science and Engineering, IOP Publishing, United Kingdom, p.012014.

Shojaee, S. and Shahri, M.M., 2016. Green synthesis and characterization of iron oxide magnetic nanoparticles using Shanghai white tea (Camelia sinensis) aqueous extract. *Journal of Chemical and Pharmaceutical Research*, 8, pp.138-143.

Sobh, R.A., Nasr, H. and Mohamed, W.S., 2020. Synthesis and characterization of magnetic sponge nanocomposite for cleaning archeological lime stones. *Egyptian Journal of Chemistry*, 63, pp.507-514.

Sravanthi, K., Ayodhya, D. and Swamy, P.Y., 2019. Green synthesis, characterization and catalytic activity of 4-nitrophenol reduction and formation of benzimidazoles using bentonite supported zero valent iron nanoparticles. *Materials Science for Energy Technologies*, 2, pp.298-307.

Yew, Y.P., Shameli, K., Miyake, M., Kuwano, N., Khairudin, N.B.B., Mohamad, S.E.B. and Lee, K.X., 2016. Green synthesis of magnetite (Fe 3 O 4) nanoparticles using seaweed (*Kappaphycus alvarezii*) extract. *Nanoscale Research Letters*, 11, pp.1-7.

Yusefi, M., Shameli, K., Yee, O.S., Teow, S.Y., Hedayatnasab, Z., Jahangirian, H., Webster, T.J. and Kuča, K., 2021. Green synthesis of Fe3O4 nanoparticles stabilized by a Garcinia mangostana fruit peel extract for hyperthermia and anticancer activities. *International Journal of Nanomedicine*, 16, p.2515.

Zhang, Q., Zhang, T., He, T. and Chen, L., 2014. Removal of crystal violet by clay/PNIPAm nanocomposite hydrogels with various clay contents. *Applied Clay Science*, 90, pp.1-5.

Zhen, G., Muir, B.W., Moffat, B.A., Harbour, P., Murray, K.S., Moubaraki, B., Suzuki, K., Madsen, I., Agron-Olshina, N. and Waddington, L., 2011. Comparative study of the magnetic behavior of spherical and cubic superparamagnetic iron oxide nanoparticles. *The Journal of Physical Chemistry C*, 115, pp.327-334.